Int J Adv Manuf Technol (2011) 52:887–895
DOI 10.1007/s00170-010-2789-x

ORIGINAL ARTICLE

Numerical analysis of chip formation and shear localisation processes in machining the Ti-6Al-4V titanium alloy

M. Calamaz · D. Coupard · M. Nouari · F. Girot

Received: 29 January 2010 / Accepted: 15 June 2010 / Published online: 25 June 2010

Abstract A finite element modelling was carried out to analyse the chip morphology and adiabatic shear banding localisation processes when high-speed machining refractory titanium alloys. A thermo-visco-plastic model for the machined material and a rigid with thermal behaviour for the cutting tool were assumed. The study tries to understand the effect of the material behaviour on the produced chip morphology. One of the main characteristics of titanium chips is a segmented shape for a wide range of cutting conditions. This kind of morphology was found only dependent on adiabatic shear banding without material damage effect in the shear zones (primary and secondary shear zones). The influence of the material characteristics (strain softening, thermal softening, etc.) and machining parameters on the cutting forces and chip morphology were analysed. Three flow-stress laws and different friction coefficients (low and high friction) at the tool-chip interface was particularly analysed to explain the different morphologies obtained for refractory titanium chips.

M. Calamaz · D. Coupard · F. Girot
Laboratoire Matériaux Endommagement Fiabilité Ingénierie des Procédés (LAMEFIP) ENSAM, CER Bordeaux,
Esplanade des Arts et Métiers,
33405 Talence Cedex, France

M. Nouari
Laboratoire d'Énergétique et de Mécanique Théorique et Appliquée, LEMTA CNRS-UMR 7563, GIP-InSIC,
27 rue d'Hellieule,
88100 Saint-Dié-des-Vosges, France

M. Nouari (✉)
Ecole Nationale Supérieure des Mines de Nancy (ENSMN),
GIP-InSIC,
27 rue d'Hellieule,
88100 Saint-Dié-des-Vosges, France
e-mail: mohammed.nouari@insic.fr

Keywords Machining · Refractory alloys · Finite element method · Shear bands · Chip segmentation · Ti-6Al-4V

1 Introduction

Machining processes are frequently used in industry to achieve parts having complex forms with high-dimensional accuracy. The Ti-6Al-4V titanium alloy is characterised by a combination of high mechanical resistance and tenacity. It is also considered as an outstanding material for aircraft industry due to its high fatigue and corrosion resistance. However, this material is well known to be difficult to machine. One of the reasons is related to its low thermal conductivity which gives rise to:

- high temperature and pressure at the tool/chip interface,
- plastic instability localised in adiabatic shear bands,
- tool wear by thermal fatigue and diffusion process.

The high chemical reactivity with many tool materials and the weak elastic modulus, which generates harmful vibrations for the tool-workpiece structure, also contribute to the low machinability of this aeronautical material.

Under high cutting speeds, many materials produce segmented chips. The Ti-6Al-4V titanium alloy is one of the particular materials which generate segmented chips (also called "saw-tooth chips") at relatively low cutting speeds [1]. The chip segmentation affects the machining process in terms of cutting forces, temperature and workpiece surface quality, thus a better knowledge of this phenomenon is needed. Two theories about segmented chip formation predominate in machining literature, namely (1) the thermoplastic instability and (2) the initiation and propagation of cracks from the outer surface of the material. Shaw et al. [2], and Komanduri and Turkovich [3] explain

that this kind of chip morphology is due to an instability occurring during the cutting process. The results from a competition between two processes were: thermal softening process and work hardening process in the primary shear zone. Vyas and Shaw [4], and Hua and Shivpuri [5] confirmed that the chip segmentation is due to a crack initiation followed by crack propagation inside the primary shear zone.

The cutting speed (V_c) and the feed (f) are the main parameters controlling the shear banding process in the chip [6]. According to Bayoumi and Xie [6], the chip load (defined by the factor $V_c \times f$) considered for the appearance of the shear bands must be around 0.004 m²/min. On the other hand, Zhen-Bin and Komanduri [1] reported that the important parameter influencing chip segmentation is the cutting speed and suggest that a critical value of the cutting speed about 9 m/min and above which a thermo-plastic instability often takes place.

Different methods have been used to simulate saw-tooth chip formation in machining: pure deformation model [7], Johnson-Cook damage model [8–12], deformation energy-based criterion [5, 13], ductile fracture criterion [14], and more recently, Baummann–Chiesa–Johnson model [15] and Rhim et al. model [16].

In other works, Baker et al. [7] assumed a critical strain value around 0.25 below which strain hardening occurs and above which titanium alloy exhibits a strain softening. This phenomenon facilitates the chip segmentation during machining. Hua and Shivpuri [5] also introduced this phenomenon in their numerical simulations of machining the Ti-6Al-4V alloy. At room temperature, a fast strain hardening phenomenon occurs which is followed by a strain softening after a peak flow stress. As the temperature increases, both strain hardening and softening material responses are reduced. This strain softening phenomenon was identified by carrying out torsion tests at high temperature on pure aluminium [17] and on different Al–Mg–Si alloys [18]. Kassner et al. [17] confirmed that for pure aluminium, the peak stress is reached at strains less than 0.5. Increasing the strain further leads to a gradual material softening. Then, the stress will reach a nearly constant level and it becomes independent on the strain. In spite of a large amount of data, the cause of the softening is not fully understood. The suggested sources for this phenomenon would be the texture softening (a decrease of the Taylor factor), the microstructural softening, the increase of the dynamic recovery and discontinuous dynamic recrystallization. The most wide-spread theories agreed that large deformation results in a dramatic increase in the high-angle boundary areas which are annihilation sites for dislocations [17]. Pettersen [18] reported that the decrease in the flow stress is due to a change in the grain size and a new operating deformation mechanism (such as grain boundary sliding) due to the dramatic increase in the high-angle grain boundary area with increasing strain.

The recovery and/or the dynamic recrystallization have been also observed in Ti-6Al-4V titanium alloy microstructure after hot processing at temperatures beyond the β-transus temperature [19]. According to Ding and Guo [19] the dynamic rescrystallization is more pronounced when the material undergo higher strains.

The aim of this paper is to study the influence of both strain softening phenomenon and friction law on the shear localisation generating segmented chips. The properties of the workpiece material were modelled using three flow-stress laws. For each case, the effect of friction at tool-chip interface is analysed. The influence of the material and cutting parameters on forces level and chip morphology is discussed. Simulated chip morphology and cutting forces were compared with experimental data. The commercial finite element software FORGE 2005® was used to construct a 2D thermo-mechanical problem and to simulate the dry machining process of the aeronautical titanium alloy Ti-6Al-4V.

2 Material behaviour and tool-chip friction laws

The law usually used to describe the material behaviour is based on Johnson-Cook model [8–12]:

$$\sigma = (A + B\varepsilon^n)\left(1 + C\ln\frac{\dot{\varepsilon}}{\dot{\varepsilon}_0}\right)\left[1 - \left(\frac{T - T_r}{T_m - T_r}\right)^m\right] \quad (1)$$

where σ is the equivalent stress, ε the equivalent plastic strain, $\dot{\varepsilon}$ the equivalent plastic strain rate, $\dot{\varepsilon}_0$ the reference equivalent plastic strain rate, T the workpiece temperature, T_m and T_r are the material melting temperature and the room temperature, respectively.

A, B, C, n and m are the material constants identified by Hopkinson pressure bar tests at strain rates up to 10^3 s^{-1} and temperatures up to 600°C. This multiplicative law takes into account the strain effect and the strain rate hardening as well as the thermal softening effects. Eq. (1) shows rather well the material behaviour up to strain rates of 10^3 s^{-1} and strain of 0.3.

In the current numerical simulations, the Johnson-Cook law was modified and implemented in the FE model to introduce the strain softening effect. The new material flow stress is given by the following equation:

$$\sigma = \left(A + B\left(\frac{1}{\dot{\varepsilon}}\right)^a \varepsilon^{\left(n - 0.12\left(\varepsilon\dot{\varepsilon}\right)^a\right)}\right)\left(1 + C\ln\left(\frac{\dot{\varepsilon}}{\dot{\varepsilon}_0}\right)\right) \times \left(1 - \left(\frac{T - T_r}{T_m - T_r}\right)^m\right) \quad (2)$$

Table 1 Parameters of the Johnson-Cook constitutive-law [8]

A (MPa)	B (MPa)	*n*	C	*m*
968	380	0.421	0.0197	0.577

The constitutive material constants used in the simulations are reported in Table 1 according to the work of Li and He [8]. When the parameter a in Eq. 2 is set to zero, the material behaviour is very close to that predicted by the non-modified Johnson-Cook model, see Fig. 1. When the parameter a is different from zero, the strain softening phenomenon appears. The higher is the value of a, the greater is the magnitude of the strain softening. Figure 2 shows the flow-stress curves when a=0.22. Three different values of a were tested in the study: a=0, a=0.11 and a=0.22. These values were not experimentally identified but arbitrarily chosen to obtain different magnitudes of the strain softening.

Figure 3 gives the flow-stress evolution versus strain rate for both material laws (Johnson-Cook and modified Johnson-Cook (MJC)) for a strain and a temperature of 0.5 and 598 K, respectively. The stress values for the MJC model correspond to the case of a=0.22. The mechanical properties of the titanium alloy are shown in Table 2. The Ti-6Al-4V thermal properties depend on temperature. The specific heat of the workpiece material varies between 565 $J(KgK)^{-1}$ at room temperature and 1,060 $J(KgK)^{-1}$ at 980°C, the thermal conductivity is about 6.6 W/mK at 20°C and 21.5 W/mK at 1,050°C. The thermal expansion coefficient takes values between 9.4×10^{-6} K^{-1} at room temperature and 1.07e-005 K^{-1} at 1,000°C.

When simulating orthogonal machining of the Ti-6Al-4V alloy, some authors [8] use a moderate friction coefficient (about 0.3) and others neglect the effect of this parameter at the tool-chip interface [20]. In the current study, friction at the tool-chip interface is controlled by Coulomb law. Two arbitrary friction conditions have been chosen: low friction (μ=0.05 for sliding contact) and high friction (μ=2 for sticking contact) to show the effect of extreme friction coefficients on the numerical results. The heat generated by friction at the tool/chip interface is dissipated inside these two bodies according to their respective effusivities. Thermal exchanges were considered between (a) the tool and the workpiece through a heat exchange coefficient h_{tw} and (b) the workpiece and the environment through another exchange coefficient h_{we}.

The workpiece structure was discretised using triangular elements, and an automatic remeshing procedure, based on mesh topology improvement [21], was used to avoid excessive element distortion induced by the cutting process. A very thin mesh (about 5 μm) was defined close to the cutting edge and along the primary shear zone to produce shear localisation and shear bands. The material separation at the tool tip is also managed by the automatic remeshing.

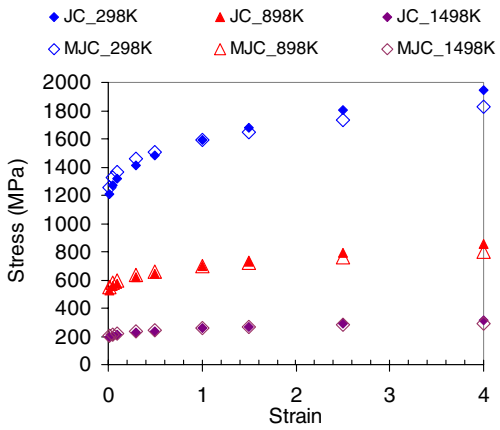

Fig. 1 Flow-stress curves for Johnson-Cook (*JC*) and modified Johnson-Cook (*MJC*) models at a strain rate of 10^5 s^{-1} for different temperatures

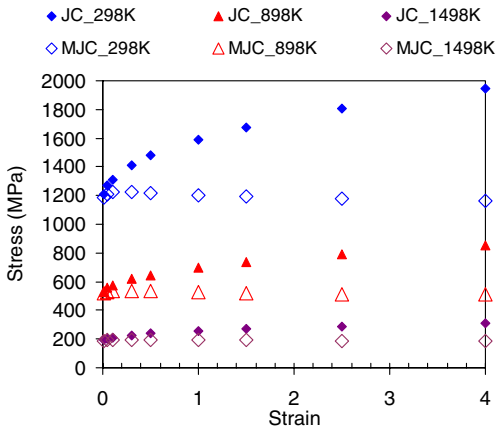

Fig. 2 Flow-stress curves for Johnson-Cook (*JC*) and modified Johnson-Cook (*MJC*) model at a strain rate of 10^5 s^{-1} for different temperatures

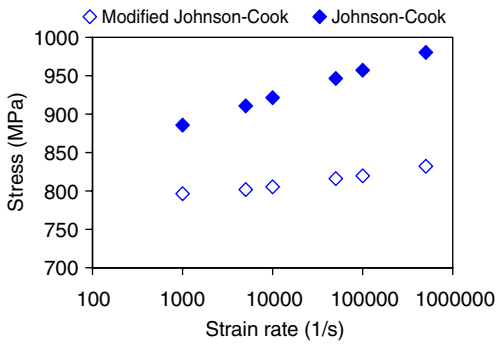

Fig. 3 Flow-stress curves for Johnson-Cook (*JC*) and modified Johnson-Cook (*MJC*) models at a temperature of 598 K and a strain of 0.5 for different strain rates

Table 2 Mechanical proprieties of the titanium alloy Ti-6Al-4V

Tensile stress (MPa)	Yield stress (MPa)	Elongation (%)	Reduction in area (%)	Young modulus (GPa)	Hardness (HV)	Density (g/cm^3)
931	862	10	25	110	340	4.43

Table 3 Different configurations of numerical simulations

Simulation	Material law parameter a	Friction coefficient μ
1	0	0.05
2	0	2
3	0.11	0.05
4	0.11	2
5	0.22	0.05
6	0.22	2

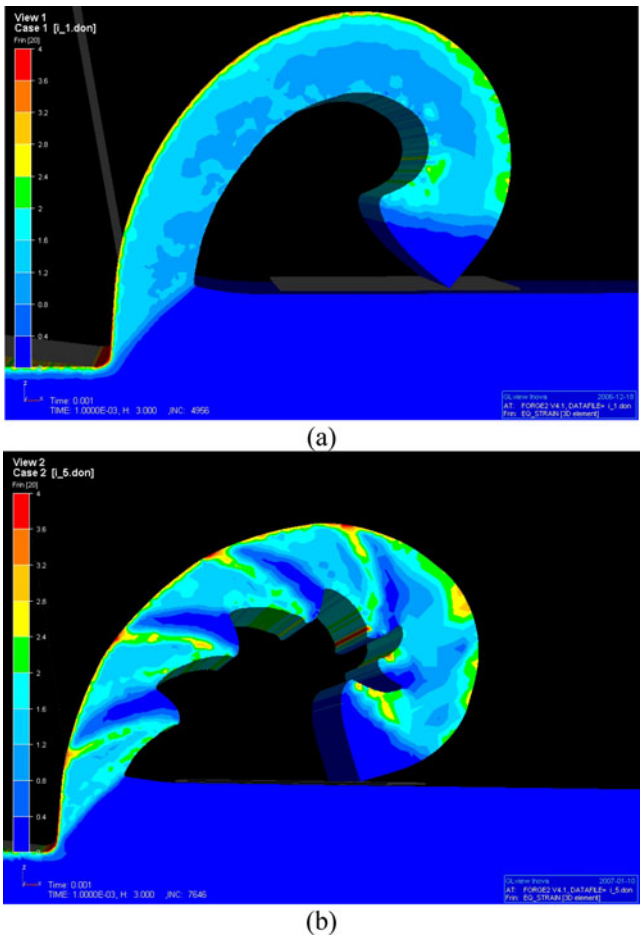

Fig. 4 Numerical chips obtained with cutting conditions: cutting speed=60 m/min and feed=0.1 mm. Friction coefficient=0.05; **a** simulation 1, a=0; **b** simulation 5, a=0.22

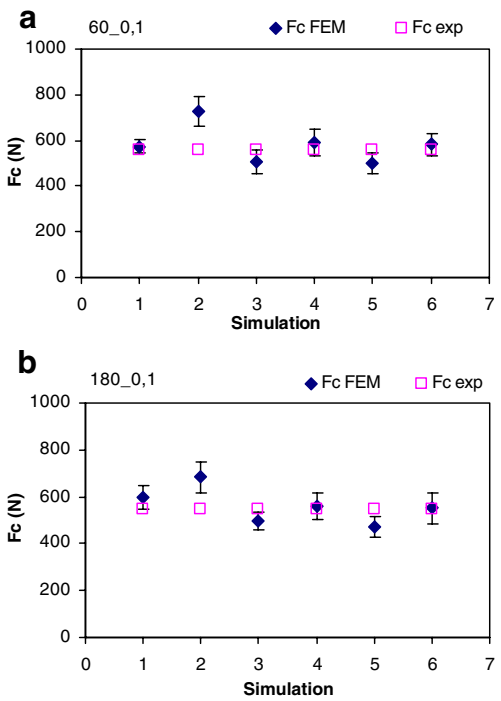

Fig. 5 Experimental and FEM cutting forces (Fc). **a** Cutting speed=60 m/min, feed=0.1 mm; **b** cutting speed=180 m/min, feed=0.1 mm

The tool discretisation would increase the size of the problem and therefore the computation time. Thus, the simulations are often carried out by considering a rigid tool to which the cutting speed V_c is imposed. In the present study, this approach was also followed. In all simulations, the cutting length is fixed to 1 mm to reduce the computation time.

3 Experimental details

Several experimental tests were carried out under orthogonal dry turning. The α-β titanium alloy Ti-6Al-4V was selected as a workpiece material. The uncoated alloyed

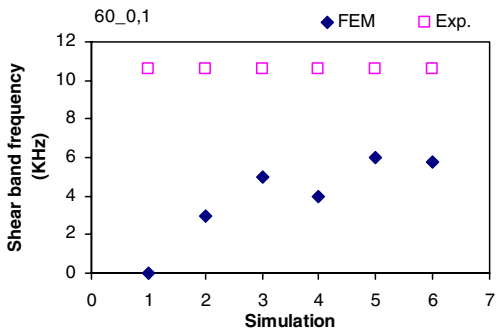

Fig. 6 Experimental and numerical chip segmentation frequency vs. numerical simulation conditions. Cutting speed=60 m/min; feed=0.1 mm

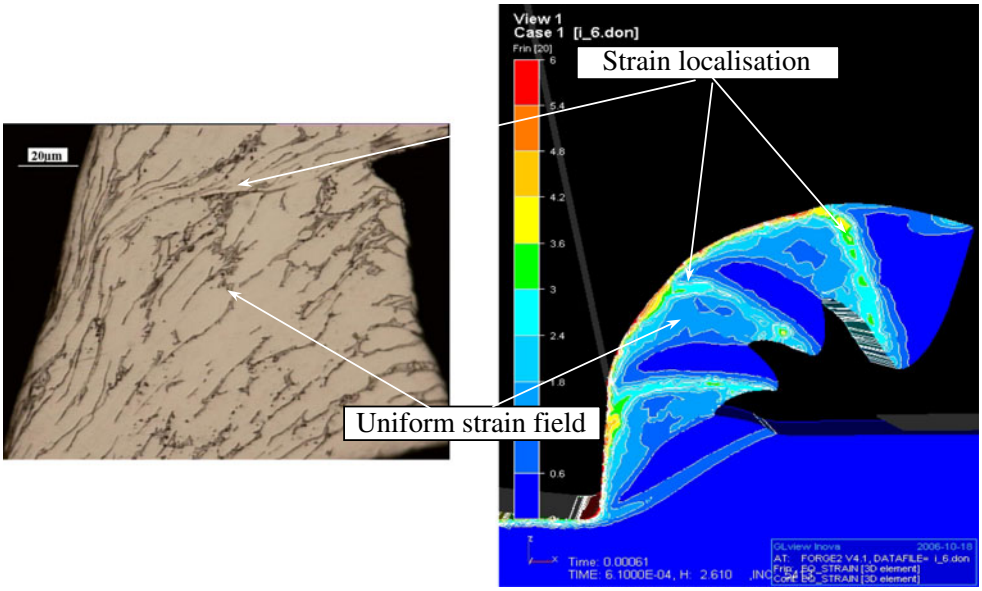

Fig. 7 **a** Experimental and **b** simulated chips obtained with a cutting speed of 60 m/min and a feed of 0.1 mm. Numerical chip corresponds to the simulation 6

carbide W-Ti/Ta/Nb-C-Co wastested with the geometry defined by a rake angle of −4°, a clearance angle of 7° and a tip radius of 20 µm. Four cutting conditions were considered: two cutting speeds (60 and 180 m/min) and two feeds (0.1 and 0.2 mm) for both orthogonal turning experiments and numerical simulations. The depth of cut was 3 mm for each experimental test. For each cutting condition, six simulation tests were made by varying the parameter a and the friction coefficient µ as illustrated in Table 3.

4 Numerical and experimental results

Figure 4a, b show the strain field of chips corresponding to simulations 1 and 5, respectively. The cutting speed of 60 m/min and the feed of 0.1 mm were chosen. The use of Johnson-Cook law (simulation 1) shows a uniform strain field and a continuous chip (Fig. 4a). When the strain softening (simulations 3, 4, 5, 6) is introduced via the parameter a in the modified Johnson-Cook model (Eq. 2), the shear localisation and chip segmentation can clearly be observed (Fig. 4b). A comparison between experimental data and simulated cutting forces under the same cutting condition is done in Fig. 5a. A good correlation can be noted for simulations 1, 4 and 6 and only simulation 2 shows a difference with a minimum mismatch of 150 N.

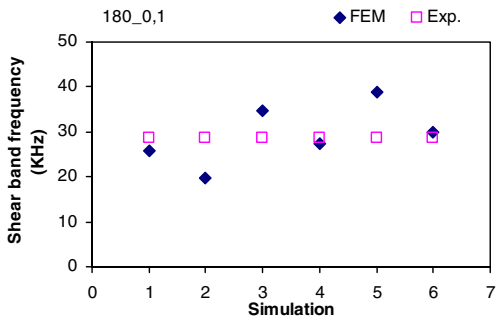

Fig. 8 Experimental and numerical chip segmentation frequency vs. numerical simulation conditions. Cutting speed=180 m/min; feed=0.1 mm

Increasing the cutting speed to 180 m/min in Fig. 5b, give the same tendency. Based on both chip morphology and cutting forces, it is clear that the Johnson-Cook model (simulations 1 and 2) cannot well correlate with experimental results. For low friction coefficient (simulation 1), i.e. sliding contact, the cutting force agrees with experiments but not the chip morphology. For high friction coefficient, i.e. sticking contact (simulation 2), the predicted cutting forces are not in a good agreement with experimental data. For simulations 3–6, when the modified Johnson-Cook model is used, chip segmentation and cutting forces are correctly predicted.

The chip segmentation frequency under the same cutting conditions has also been analysed, see Fig. 6. The worst results were obtained with Johnson-Cook law (simulations 1 and 2) giving a continuous chip (simulation 1) or a low chip segmentation frequency (simulation 2). The use of the Modified Johnson-Cook law in simulations 3–6 enables higher chip frequencies especially for cases 5 and 6 which correspond to higher values of a, i. e. a higher degree of strain softening. The mismatch between experimental and simulated chip frequencies should result from an incorrect modelling of the flow stress in the range of strain rate and temperature obtained under such cutting conditions.

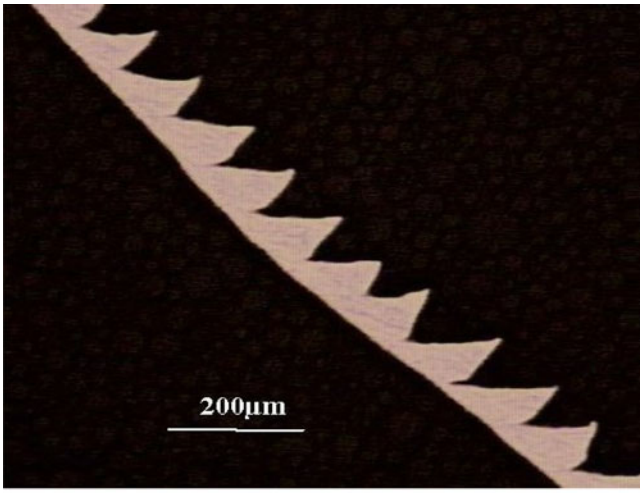

a

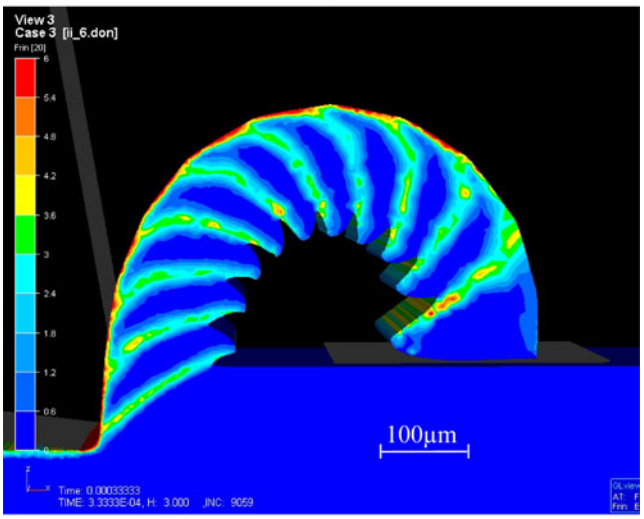

b

Fig. 9 **a** Experimental and **b** simulated chips. Cutting conditions: cutting speed=180 m/min; feed=0.1 mm. Simulated chip corresponds to simulation 6

Figure 7 shows a comparison between experimental and simulated chips under the same cutting conditions. Figure 7b is related to simulation 6 with a friction coefficient of 2 and material parameter *a* of 0.22. It is interesting to observe the similar strain distribution in the simulated and real chip. For both cases, two different strain regions can clearly be identified: the primary shear zone in which a strong strain localisation occurs and a quite uniform strain zone.

Figure 8 compares the experimental and simulated chip segmentation frequencies when using a high cutting speed (about 180 m/min) and the same feed (0.1 mm). When increasing the cutting speed from 60 to 180 m/min, the chip segmentation frequency can be predicted accurately whatever the simulation considered. A good correlation is especially obtained when using a high friction coefficient associated to a high value of the parameter *a* (simulations 4 and 6 of Fig. 8). Moreover, the cutting forces were also correctly predicted (see Fig. 5b). Under these cutting conditions, the Johnson-Cook model enables segmented chip to be predicted whatever the friction coefficient value, contrary to previous case (60 m/min–0.1 mm). Figure 9a, b show micrographs of a real chip and the strain field of the simulated chip (simulation 6) obtained for a cutting speed of 180 m/min and a feed of 0.1 mm. In both cases, ten segments were obtained over a cutting length of 1 mm.

Figure 10a, b compare the microstructure of an etched chip with the simulated strain field when using a cutting speed of 60 m/min and a feed of 0.2 mm. The maximum strain value in Fig. 10b is set to 6, as for Fig. 7b. In this case, it can be noted that no uniform deformation zone appears. The deformation is mainly concentrated in narrow bands between low deformed segments. The strain inside the primary shear zone is also higher than that shown in Fig. 7b. When increasing the feed to 0.2 mm, the correlation between experimental and simulated results is quite close to that observed for a cutting speed of 180 m/min with a feed of 0.1 mm. Figure 11 compares the experimental and simulated cutting forces for cutting speeds of 60 and 180 m/min with a feed of 0.2 mm while Figs. 12 and 13 give the chip segmentation frequency under the same conditions. According to Fig. 11, the correlation between simulated and experimental cutting forces is fairly good except for simulation 2 corresponding to the Johnson-Cook model and high friction coefficient. According to Figs. 12 and 13, the best correlation is obtained for simulation 4 confirming the accuracy of the modified Johnson-Cook model.

The numerical simulation with the material parameter *a* set to 0.11 and the sticking contact at the tool-chip interface shows a quite good correlation for both cutting forces and chip segmentation frequency (see Figs. 11, 12 and 13).

The nature of the friction contact between the chip and the tool is an important parameter to consider in machining simulation. As it can be seen in Figs. 5a, b and 11a, b, the cutting forces are not sensitive to the friction coefficient when the machining process is simulated with the MJC law (simulations 3–6). The simulated data with the Johnson-Cook law (simulations 1 and 2 in Fig. 5a, b) are affected by the change of the contact conditions. The friction coefficient modifies the shear band frequency and especially the level of the generated temperature at the tool-chip interface. The produced temperature increases when the sticking contact ($\mu=2$) is assumed. As it can be seen in Figure 14a, b, for a cutting speed of 180 m/min and a feed of 0.1 mm, the simulated interface temperature will increase from 700°C for the low friction coefficient to 900°C when using the high friction coefficient.

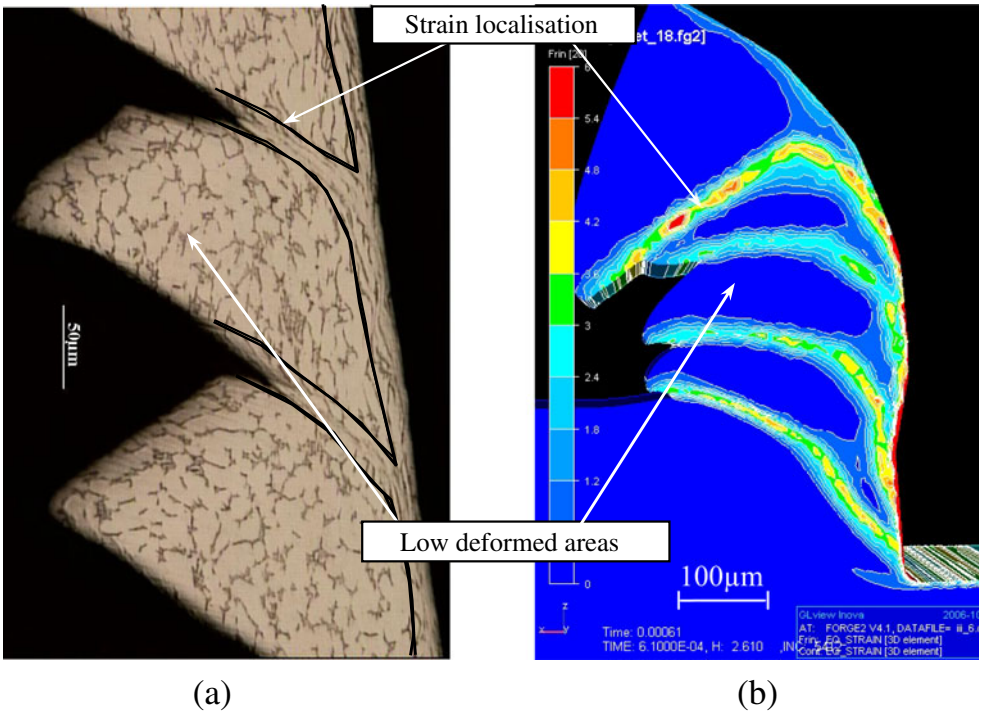

Fig. 10 **a** Experimental and **b** simulated chips obtained with a cutting speed of 60 m/min and a feed of 0.2 mm. Simulated chip corresponds to simulation 6

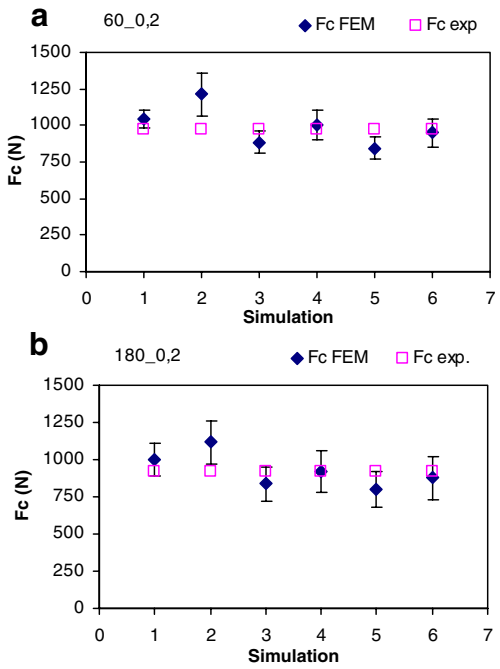

Fig. 11 Experimental and FEM cutting forces (*Fc*). **a** Cutting speed=60 m/min, **b** cutting speed=180 m/min; feed=0.2 mm

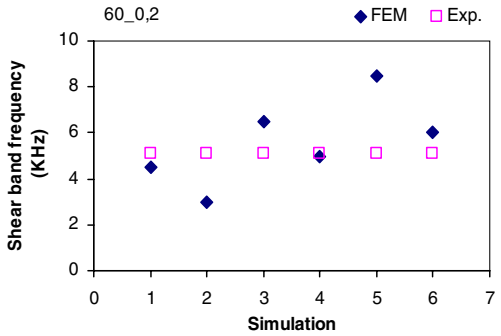

Fig. 12 Experimental and numerical chip segmentation frequencies vs. numerical simulation conditions; cutting speed=60 m/min; feed=0.2 mm

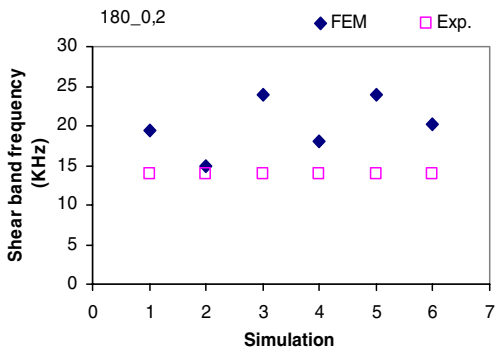

Fig. 13 Experimental and numerical chip segmentation frequencies vs. numerical simulation conditions; cutting speed=180 m/min; feed=0.2 mm

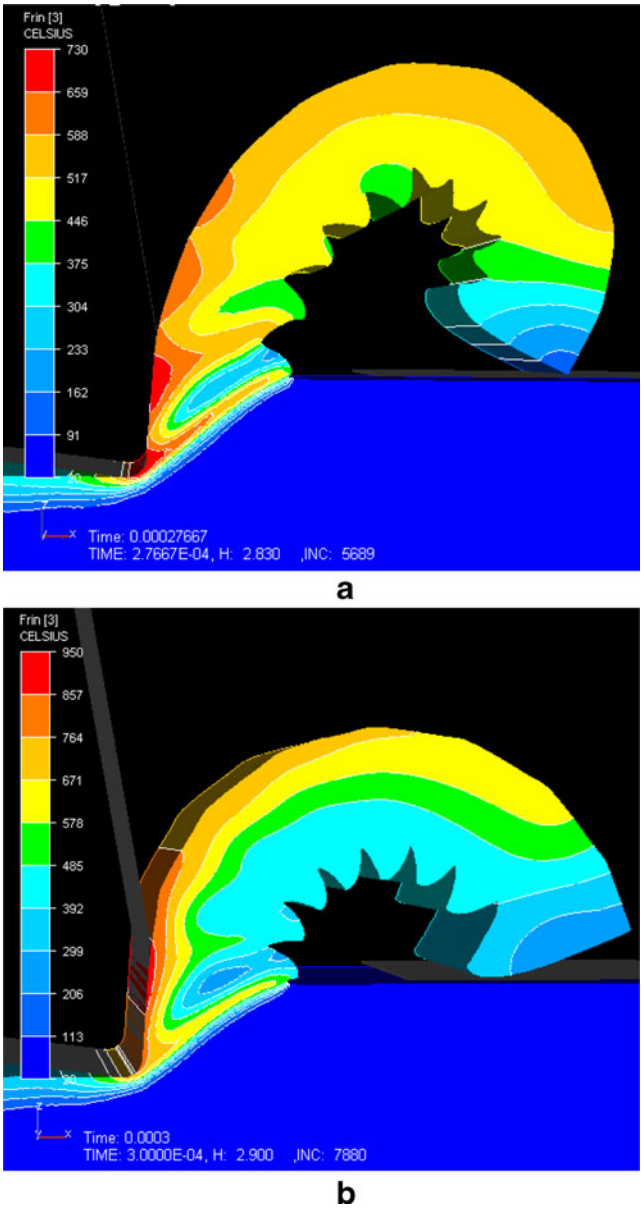

Fig. 14 Temperature distribution for a simulation with a **a** sliding and **b** sticking contact. The simulation conditions are: cutting speed= 180 m/min and feed=0.1 mm. Simulated chips correspond to simulations 3 and 4

5 Conclusions

The material behaviour and friction laws between the cutting tool and the workpiece are the main parameters to be taken carefully to obtain accurate results with numerical simulations. In machining process, a good numerical model starts with a correct prediction of the chip morphology and cutting parameters such as cutting forces, temperature and contact pressure. For all cutting conditions, the assumed thermoviscoplastic model in this work is able to give a good prediction of chip morphology, segmentation frequency and cutting forces. A best agreement was obtained when using a high value of the friction coefficient together with the introduced strain softening parameter a of 0.11. Also the strain distribution into the simulated chip is in good agreement with the deformed microstructure of the chip obtained by experimental tests. The study has been shown that the cutting forces are not sensitive to the nature of the friction contact between the chip and the tool during the machining process. The friction coefficient affects the shear band frequency and the tool-chip interface temperature.

Acknowledgements The authors wish to thank Jacques GERAUD and Frédéric LALARDIE for their help in the present work and for conducting part of experiments.

Research support was provided by the French Department of Education and Science trough the contract n°02 K0538 (MEDOC project).

References

1. Zhen-Bin H, Komanduri R (1995) On a thermo-mechanical model of shear instability in machining. Ann CIRP 44(1):69–73
2. Shaw MC, Dirke SO, Smith PA, Cook NH, Loewen EG, Yang CT (1954) Machining titanium, Massachusetts Institute of Technology, Cambridge, MA, USA
3. Komanduri R, Turkovich BF (1981) New observations on the mechanism of chip formation when machining titanium alloys. Wear 69:179–188
4. Vyas A, Shaw MC (1999) Mechanics of saw-tooth chip formation in metal cutting. J Manufact Sci Eng 121:165
5. Hua J, Shivpuri R (2004) Prediction of chip morphology and segmentation during the machining of titanium alloys. J Mater Process Technol 150:124–133
6. Bayoumi AE, Xie JQ (1995) Some metallurgical aspects of chip formation in cutting Ti-6 wt.% Al-4 wt.%V alloy. Mater Sci Eng Abstr 190:173–180
7. Baker M, Rösler J, Siemers C (2002) A finite element model of high speed metal cutting with adiabatic shearing. Comput Struct 80(5–6):495–513
8. Li L, He N (2006) A FEA study on mechanisms of saw-tooth chip deformation in high speed cutting of Ti-6-Al-4 V alloy. In: Proceedings of the Fifth International conference on High Sped Machining, Metz, France. pp 759–767
9. Arrazola PJ, Ugarte D, Villar JA, Marya S (2006) Finite element modelling: a qualitative tool to study high speed machining. In: Proceedings of the Fifth International conference on High Sped Machining, Metz, France
10. Barge M, Hamdi H, Rech J, Bergheau J-M (2005) Numerical modelling of orthogonal cutting: influence of numerical parameters. J Mater Process Technol 164:1148–1153
11. Pantalé O, Bacaria J-L, Dalverny O, Rokotomalala R, Caperaa S (2004) 2D and 3D numerical models of metal cutting with damage effects. Comput Meth Appl Mech Eng 193:4383–4399
12. Guo YB, Yen DW (2004) A FEM study on mechanisms of discontinuous chip formation in hard machining. J Mater Process Technol 155–156:1350–1356
13. Ceretti E, Lucchi T, Altan T (1999) FEM simulation of orthogonal cutting: serrated chip formation. J Mater Process Technol 95:17–26

14. Obikawa T, Usui E (1996) Computational machining of titanium alloy-finite element modelling and a few results. Trans Am Soc Mech Eng 118:208–215
15. Guo YB, Wen Q, Woodbury KA (2006) Dynamic material behavior modelling using internal state variable plasticity and its application in hard machining simulations. J Manuf Sci Eng 128:749–756
16. Rhim S-H, Oh S-I (2006) Prediction of serrated chip formation in metal cutting process with new flow stress model for AISI 1045 steel. J Mater Process Technol 171:417–422
17. Kassner ME, Wang MZ, Perez-Prado M-T, Alhajeri S (2002) Large-strain softening of aluminium in shear at elevated temperature. Metall Mater Trans A 33A:3145–3153
18. Pettersen T, Nes E (2003) On the origin of strain softening during deformation of aluminium in torsion to large strains. Metall Mater Trans A 34A:2727–2736
19. Ding R, Guo ZX (2004) Miscrostructural evolution of a Ti-6Al-4V alloy during β-phase processing: experimental and simulative investigations. Mater Sci Eng A365:172–179
20. Baker M (2006) Finite element simulation of high-speed cutting forces. J Mater ProcessTechnol 176:117–126
21. Gruau C, Coupez T (2003) Anisotropic and multidomain mesh automatic generation for viscous flow finite element method. In: Proceedings of the International conference on Adaptative and Modeling Simulation (ADMOS 03), Goteburg, Sweden